Inorg. Chem. **2003**, *42*, 2968–2976

Synthesis, Crystal Structures, and Thermal and Thermodynamic Properties of Dimorphic Copper(I) Coordination Polymers

Christian Näther* and Inke Jess

Kiel, Institut für Anorganische Chemie der Christian-Albrechts-Universität, Olshausenstrasse 40, D-24098 Kiel, Germany

Received November 15, 2002

A second modification of the literature-known copper(I) coordination polymer CuCl(pyridazine) was prepared by the reaction of CuCl with pyridazine in acetonitrile. The crystal structure of catena[CuCl(μ_2-pyridazine-*N*,*N*)] is built up of CuCl chains of which each two are connected by the pyridazine ligands to form double chains that are directed parallel to the crystallographic *a*-axis. In the literature known form **LI** $(CuCl)_2$ dimers occur that are connected to chains by the pyridazine ligand. On heating, compound **I** and **LI** lose half of the pyridazine ligands and transform to the new 2:1 coordination polymer poly[$(CuCl)_2$(pyridazine-*N*,*N*)] (**II**), which transforms at higher temperatures to CuCl. The crystal structure of **II** is composed of discrete CuCl tetra-chains that are linked by the pyridazine ligands to sheets parallel to (010). The same thermal reactivity is found for the literature-known compound CuBr(pyridazine) (**LII**), which is isotypic to **LI**. On heating **LII** a transformation into the new 2:1 compound poly[$(CuBr)_2$(pyridazine-*N*,*N*)] (**III**) is observed, which is isotypic to **II**. The thermal reactivity of all compounds and the transformation behavior as well as the range of thermodynamic stability of the dimorphic modifications were studied using DTA–TG–MS and DSC measurements, temperature dependent X-ray powder investigations, and crystallization experiments.

Introduction

Recently, the development of strategies for a more directed construction of new coordination architectures in order to prepare compounds with interesting physical properties has been a special field of interest.[1−15] This approach, called "crystal engineering", must include a special knowledge of the interactions in crystals as well as the structure−property relationships in solids.[16] However, the small differences in energies between different crystalline modifications lead frequently to polymorphism, which is defined as the ability of a compound to crystallize in more than one modification.[16,17] Therefore, this phenomenon was described as the "Nemesis of crystal design". Besides polymorphism also isomerism is frequently found in coordination compounds.[4,18−20] The term isomerism, like, for example, structural isomerism or supramolecular isomerism, is much more

* Author to whom correspondence should be addressed. E-mail: cnaether@ac.uni-kiel.de.

(1) Batten, S. R.; Robson, R. *Angew. Chem.* **1998**, *110*, 1558−1595; *Angew. Chem., Int. Ed.* **1998**, *37*, 1460−1467.
(2) Blake, A. J.; Champness, N. R.; Hubberstey, P.; Li, W.-S.; Schröder, M. *Coord. Chem. Rev.* **1999**, *183*, 17−33.
(3) Robson, R.; Abrahams, B. F.; Batten, S. R.; Grable, R. W.; Hoskins, B. F.; Liu, J. In *Supramolecular Architecture*; American Chemical Society: Washington, DC, 1992; Chapter 19.
(4) Moulton, B.; Zaworotko, M. *J. Chem. Soc. Rev.* **2001**, *101*, 1629−1658.
(5) Zaworotko, M. J. *Angew. Chem.* **2000**, *112*, 3180−3182; *Angew. Chem., Int. Ed.* **2000**, *39*, 3052−3054.
(6) Robson, R. *Compr. Supramol. Chem.* **1996**, *22*, 733−748.
(7) Yaghi, O. M.; Li, H.; Davis, C.; Richardson, D.; Groy, T. L. *Acc. Chem. Res.* **1998**, *31*, 474−484.
(8) Hagrman, P. J.; Hagrman, D.; Zubieta, J. *Angew. Chem.* **1999**, *111*, 2798−2848; *Angew. Chem., Int. Ed.* **1999**, *38*, 2638−2688.
(9) Batten, S. R.; Jeffery, J. C.; Ward, M. D. *Inorg. Chim. Acta* **1999**, *292*, 231−237.
(10) Kutasi, A. M.; Batten, S. R.; Harris, A. R.; Moubaraki, B.; Murray, K. S. *CrystEngComm* **2002**, 202−204.
(11) Holiday, B. J.; Mirkin, C. A. *Angew. Chem.* **2001**, *113*, 2076−2098; *Angew. Chem., Int. Ed.* **2001**, *40*, 2022−2044.
(12) Batten, S. R.; Hoskins, B. F.; Robson, R. *Chem. Eur. J.* **2000**, *6* (1), 156−161.
(13) Chesnut, D. J.; Kusnetzow, A.; Zubieta, J. *J. Chem. Soc., Dalton Trans.* **1998**, 4081−4083.
(14) Manson, J. L.; Arif, A. M.; Miller, J. S. *Chem. Commun.* **1999**, 1479−1480.
(15) Reineke, T. M.; Eddaoudi, M.; O'Keeffe, O.; Yaghi, O. M. *Angew. Chem.* **1999**, *111*, 2712−2716; *Angew. Chem., Int. Ed.* **1999**, *38*, 2590−2594.
(16) Desiraju, G. R. *Crystal Engineering—The Design of Organic Solids*; Material Science Monographs; Elsevier: Amsterdam, 1989; Vol. 54 and literature cited therein.
(17) Bernstein, J.; Davey, R.; Henck, O. *Angew. Chem.* **1999**, *111*, 3646; *Angew. Chem., Int. Ed.* **1999**, *38*, 3440.
(18) Batten, S. R.; Murray, K. S. *Aust. J. Chem.* **2001**, *54*, 605−609.

10.1021/ic026181i CCC: $25.00
Published on Web 04/03/2003

strongly defined and considers also differences in the coordination of the building blocks and the network architecture in coordination polymers. As for polymorphism this special arrangement is coupled to the solid state and will probably not exist in solution. Therefore, polymorphism should also include isomerism. From the viewpoint of a "crystal engineer" both phenomena are of special importance, because they provide information on intermolecular interactions in coordination polymers and can therefore lead to a more rational crystal design. Besides these structural aspects of these phenomena also investigations on the transformation behavior and the kinetic and thermodynamic aspects are necessary in order to draw structure−property relationships.[17,21−24]

Recently, we have found polymorphic modifications in coordination polymers based on copper(I) halides or pseudohalides and multidendate N-donor ligands.[24] The structures of such coordination polymers are built up of different CuX substructures (X = halide or pseudohalide) which are linked by the organic ligands to multidimensional coordination polymers.[24−43] For one definite copper(I) halide or pseudohalide and one specific N-donor ligand often several compounds can be prepared, which contain a different CuX: ligand ratio like, e.g., 1:2, 1:1, 3:2, 2:1, or 4.1. We have found that most of the ligand-rich compounds can be transformed into ligand-poorer compounds by thermal decomposition, which is an alternative route for the preparation of new CuX coordination polymers.[36−43]

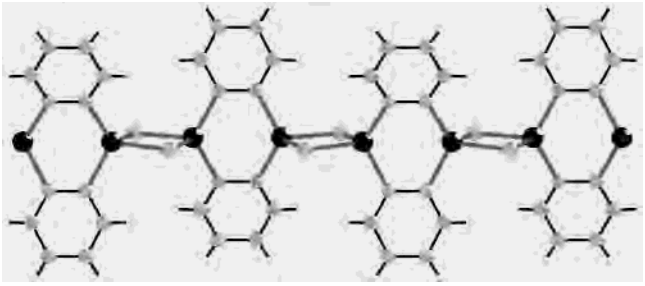

Figure 1. Crystal structure of form **LI** of catena[CuCl(μ_2-pyridazine)] with view perpendicular to the chains.

During our systematic investigations on the thermal behavior of such CuX coordination polymers, we have also investigated the CuX compounds (X = Cl, Br) with pyridazine. The 1:1 compounds CuX(pyridazine) (X = Cl (**LI**) and X = Br (**LII**)) were published recently.[29] Both compounds are isotypic and crystallize in the orthorhombic space group *Cmca* with 16 formula units in the cell. Their crystal structures are built up of $(CuX)_2$ dimers, which are connected into chains by the pyridazine ligands (Figure 1).

For the investigations of the thermal properties of these compounds we have tried to prepare pure **LI** and **LII**, but for **LI** the experimental powder pattern does not correspond to that calculated from single-crystal data. However, by systematic investigations we have isolated crystals of this additional compound, which represents a second modification of **LI**. In addition, we prepared all 1:1 phases and have investigated their thermal properties. Here we report the results of these investigations.

Experimental Section

Synthesis of Catena[CuCl(μ_2-pyridazine-*N*,*N*)] (I). The thermodynamically most stable modification **I** was prepared by the reaction of 98.98 mg (1.0 mmol) of CuCl and 80.09 mg (1.0 mmol) of pyridazine in 3 mL of acetonitrile at 120 °C in a sealed glass ampule for 3 days. The residue consisted of red needles suitable for X-ray single-crystal structure analysis, which were filtered off and washed with diethyl ether. During cooling the product should not have any contact with the saturated solution. Otherwise a few crystals of **LI** were formed. Yield: 71.1%. Elemental anal. Calcd: C, 26.83; N, 15.64; H, 2.25. Found: C, 26.61; N, 15.43; H, 2.11. X-ray powder diffraction: phase pure. The reaction can also be performed at room temperature. In this case the reaction mixture must be stirred for about 1 day until the metastable form **LI** is transformed into the stable form **I**.

Synthesis of Catena[CuCl(μ_2-pyridazine-*N*,*N*)] (LI). The literature-known compound **LI** is metastable in the complete temperature range investigated and can be prepared only if the synthesis is performed under kinetic control. If a saturated solution of CuCl in acetonitrile is added to a solution of pyridazine in acetonitrile with stirring, a red precipitate is formed, which must be immediately filtered off. Otherwise it transforms into the thermodynamically most stable form **I**. Because a saturated solution of CuCl is used, the exact stoichiometry is difficult to adjust and, therefore, no reliable yield can be given. If solid CuCl is used, the residue is always contaminated with CuCl. In addition, dependent

(19) Braga, D.; Maini, L.; Polito, M.; Scaccianoce, L.; Cojazzi, G.; Grepioni, F. *Coord. Chem. Rev.* **2001**, *216*, 783−788.
(20) Barnett, A. S.; Blake, A. J.; Champness, N. R.; Wilson, C. *Chem. Commun*. **2002**, 1640−1641.
(21) Bock, H.; Schödel, H.; Näther, C.; Butenschön, F. *Helv. Chim. Acta* **1997**, *80*, 593−605.
(22) Schödel, H.; Näther, C.; Bock, H.; Butenschön F. *Acta Crystallogr*. **1996**, *B52*, 842−853.
(23) Näther, C.; Jess, I.; Havlas, Z.; Bolte, M.; Nagel N.; Nick, S. *Solid State Sci.* **2002**, *4*, 859−871.
(24) Näther, C.; Wriedt, M.; Jess, I. *Inorg. Chem*. **2003**, *42*, 2391−2397.
(25) Blake, A. J.; Brooks, N. R.; Champness, N. R.; Cook, P. A.; Deveson, A. M.; Fenske, D.; Hubberstey, P.; Li, W.-S.; Schröder, M. *J. Chem. Soc., Dalton Trans.* **1999**, 2103−2110.
(26) Blake, A. J.; Brooks, N. R.; Champness, N. R.; Cooke, P. A.; Crew, M.; Deveson, A.; M. Hanton, L. R.; Hubberstey, P.; Fenske, D.; Schröder, M. *Cryst. Eng.* **1999**, *2*, 181−195.
(27) Blake, A. J.; Brooks, N. R.; Champness, N. R.; Hanton, L. R.; Hubberstey, P.; Schröder, M. *Pure Appl. Chem.* **1998**, *70*, 2351−2358.
(28) Rossenbeck, B.; Sheldrick, W. S. *Z. Naturforsch*. **2000**, *55b*, 467−472.
(29) Kromp, T.; Sheldrick, W. S. *Z. Naturforsch*. **1999**, *54b*, 1175−1180.
(30) Teichert, O.; Sheldrick, W. S. *Z. Anorg. Allg. Chem*. **1999**, *625*, 1860−1865.
(31) Teichert, O.; Sheldrick, W. S. *Z. Anorg. Allg. Chem*. **2000**, *626*, 1509−1513.
(32) Teichert, O.; Sheldrick, W. S. *Z. Anorg. Allg. Chem*. **2000**, *626*, 2196−2202.
(33) Persky, N. S.; Chow, J. M.; Poschmann, K. A.; Lacuesta, N. N.; Stoll, S. L. *Inorg. Chem*. **2001**, *40*, 29−35.
(34) Graham, P. M.; Pike, R. D.; Sabat, M.; Bailey, R. D.; Pennington, W. T. *Inorg. Chem*. **2000**, *39*, 5121−5132.
(35) Lu, J. Y.; Cabrera, B. R.; Wang, R.-J.; Li, J. *Inorg. Chem*. **1999**, *38*, 4608−4611.
(36) Näther, C.; Greve, J.; Jess, I. *Polyhedron* **2001**, *20*, 1017−1022.
(37) Näther, C.; Jess, I. *Monatsh.Chem.* **2001**, *132*, 897−910.
(38) Näther, C.; Jess, I.; Studzinski. H. *Z. Naturforsch*. **2001**, *56b*, 997−1002.
(39) Näther, C.; Wriedt, M.; Jess, I. *Z. Anorg. Allg. Chem*. **2002**, *628*, 394−400.
(40) Näther, C.; Greve, J.; Jess, I. *Solid State Sci.* **2002**, *4* (6), 813−820.
(41) Näther, C.; Jess, I. *J. Solid State Chem*. **2002**, *169*, 103−112.
(42) Näther, C.; Jess, I. *Z. Naturforsch*. **2002**, *57b*, 1133−1140.
(43) Kromp, T.; Sheldrick, W. S.; Näther, C. *Z. Anorg. Allg. Chem*. **2003**, *629*, 45−54.

on the reaction time the samples are always contaminated with small amounts of form **I**. We have found no access to phase pure samples of **LI**. Single crystals of **LI** were prepared at 120 °C in glass ampules. Slow cooling leads to a large amount of needlelike single crystals of **I**, which contain a few red polyhedra of form **LI**.

Synthesis of Poly[(CuCl)$_2$(pyridazine-*N*,*N*)] (II). This compound was prepared by thermal decomposition of compound **I** (see below). Yield: about 100%. Elemental anal. Calcd: C, 17.28; N, 10.07; H, 1.45. Found: C, 17.11; N, 9.93; H, 1.35. X-ray powder diffraction: phase pure. Single crystals of **II** were prepared by the reaction of 198.5 mg (2.0 mmol) of CuCl and 80.09 mg of pyridazine (1.0 mmol) in 3 mL of acetonitrile in a Teflon-lined steel autoclave at 100°C for 6 days. The reaction mixture was cooled to room temperature within 1 day. The residue is not phase pure but consists of a few orange needles of **II** suitable for X-ray single-crystal diffraction. If the reaction is performed in solution at room temperature, the product contains a mixture of compounds **I** and **II**.

Synthesis of Catena[CuBr(μ_2-pyridazine-*N*,*N*)] (LII). Copper(I) bromide (143.45 mg, 1.0 mmol) and 80.09 mg (1.0 mmol) of pyridazine were reacted in 3 mL of acetonitrile at room temperature for 1 day. The orange precipitate was filtered off and washed with ethanol and diethyl ether. Yield: 91.8%. Elemental anal. Calcd: C, 21.49; N, 12.53; H, 1.80. Found: C, 21.36; N, 12.44; H, 1.75. X-ray powder diffraction: phase pure.

Synthesis of Poly[(CuBr)$_2$(pyridazine-*N*,*N*)] (III). This compound was prepared by thermal decomposition of compound **LII**. Yield: about 100%. Elemental anal. Calcd: C, 13.09; N, 7.63; H, 1.10. Found: C, 12.98; N, 7.54; H, 1.04. X-ray powder diffraction: phase pure. Single crystals of **III** were prepared by the reaction of 286.9 mg (2.0 mmol) of CuBr and 80.09 mg (1.0 mmol) of pyridazine in 3 mL of acetonitrile in a Teflon-lined steel autoclave at 120 °C for 3 days. The reaction mixture was cooled to room temperature within 1 day. The residue is not phase pure and consists of a few orange needlelike crystals which were suitable for X-ray single-crystal diffraction. If the reaction is performed in solution at room temperature, the product consists always of a mixture of compounds **LII** and **III**.

Single-Crystal Structure Determination. For all compounds a face-indexed absorption correction using X-SHAPE[44] and XEMP[45] was applied. The structure solution was performed using SHELXS-97,[46] and structure refinement was done against F^2 using SHELXL-97.[47] All non-hydrogen atoms were refined using anisotropic displacement parameters. The hydrogen atoms were positioned with idealized geometry and refined with isotropic displacement parameters using the riding model. Details of the structure determination and lists with selected bond lengths and angles are given in Tables 1 and 2.

X-ray Powder Diffraction. X-ray powder diffraction experiments were performed using a STOE STADI P transmission powder diffractometer that is equipped with a 4° and 45° PSD (position sensitive detector) using Cu Kα radiation (λ = 1.540598 Å). The diffractometer is equipped with a graphite furnace from STOE & CIE for temperature or time dependent X-ray powder diffraction.

Table 1. Crystal Data and Results of the Structure Refinement for Catena[CuCl(μ_2-pyridazine-*N*,*N*)] (**I**), Poly[(CuCl)$_2$(pyridazine-*N*,*N*)] (**II**), and Poly[(CuBr)$_2$(pyridazine-*N*,*N*)] (**III**)

	I	**II**	**III**
chemical formula	$C_4H_4N_2CuCl$	$C_4H_4N_2Cu_2Cl_2$	$C_4H_4N_2Cu_2Br_2$
fw	179.08	278.07	366.99
space group	$P\bar{1}$	$P\bar{1}$	$P\bar{1}$
a, Å	3.7512(6)	3.7757(8)	3.9577(9)
b, Å	8.412(1)	8.687(2)	8.787(2)
c, Å	8.900(1)	11.537(2)	11.823(2)
α, deg	90.43(1)	106.03(2)	105.44(2)
β, deg	94.04(1)	95.69(2)	94.71(2)
γ, deg	92.27(1)	96.36(2)	96.17(2)
V, Å^3	279.88(7)	358.1(1)	391.4(2)
T, °C	20	20	20
Z	2	2	2
D_{calcd}, g cm^{-3}	2.125	2.579	3.114
μ, mm^{-1}	4.25	6.59	15.56
λ, Å	0.71073	0.71073	0.71073
R1[a] [$I > 2\sigma(I)$]	0.0362	0.0291	0.0273
wR2[a] [all data]	0.0952	0.0788	0.0674

[a] $R1 = \sum||F_o| - |F_c||/\sum|F_o|$; $wR2 = [\sum[w(F_o^2 - F_c^2)^2]/\sum[w(F_o^2)^2]]^{1/2}$.

Table 2. Selected Bond Lengths (Å) and Angles (deg) for Catena[CuCl(μ_2-pyridazine-*N*,*N*)] (**I**), Poly[(CuCl)$_2$(pyridazine-*N*,*N*)], (**II**) and Poly[(CuBr)$_2$(pyridazine-*N*,*N*)] (**III**)

Catena[CuCl(μ_2-pyridazine-*N*,*N*)] (**I**)			
Cu(1)−N(2A)	2.004(3)	Cu(1)−N(1)	2.026(3)
Cu(1)−Cl(1)	2.337(1)	Cu(1)−Cl(1B)	2.408(2)
Cl(1)−Cu(1C)	2.408(2)	N(2)−Cu(1A)	2.004(3)
N(2A)−Cu(1)−N(1)	120.4(2)	N(2A)−Cu(1)−Cl(1)	115.1(1)
N(1)−Cu(1)−Cl(1)	105.9(1)	N(2A)−Cu(1)−Cl(1B)	103.9(1)
N(1)−Cu(1)−Cl(1B)	105.5(1)	Cl(1)−Cu(1)−Cl(1B)	104.5(1)
Poly[(CuCl)$_2$(pyridazine-*N*,*N*)] (**II**)			
Cu(1)−N(2A)	1.990(3)	Cu(1)−N(1)	1.997(3)
Cu(1)−Cl(1)	2.354(1)	Cu(1)−Cl(1B)	2.480(2)
Cu(2)−Cl(1)	2.287(2)	Cu(2)−Cl(2C)	2.376(2)
Cu(2)−Cl(2)	2.376(2)	Cu(2)−Cl(2D)	2.458(2)
Cl(1)−Cu(1C)	2.480(2)		
N(2A)−Cu(1)−N(1)	124.06(11)	N(2A)−Cu(1)−Cl(1)	115.50(9)
N(1)−Cu(1)−Cl(1)	106.83(9)	N(2A)−Cu(1)−Cl(1B)	100.92(9)
N(1)−Cu(1)−Cl(1B)	103.70(9)	Cl(1)−Cu(1)−Cl(1B)	102.69(4)
Cl(1)−Cu(2)−Cl(2)	114.58(4)	Cl(1)−Cu(2)−Cl(2C)	113.93(4)
Cl(2)−Cu(2)−Cl(2C)	99.56(4)	Cl(1)−Cu(2)−Cl(2C)	119.42(4)
Cl(2)−Cu(2)−Cl(2D)	105.22(4)	Cl(2)−Cu(2)−Cl(2D)	102.05(4)
Poly[(CuBr)$_2$(pyridazine-*N*,*N*)] (**III**)			
Cu(1)−N(2A)	2.001(3)	Cu(1)−N(1)	2.006(3)
Cu(1)−Br(1)	2.472(1)	Cu(1)−Br(1B)	2.586(1)
Cu(2)−Br(1)	2.449(1)	Cu(2)−Br(2C)	2.508(1)
Cu(2)−Br(2)	2.500(1)	Cu(2)−Br(2D)	2.535(1)
Br(1)−Cu(1C)	2.586(1)		
N(2A)−Cu(1)−N(1)	123.86(12)	N(2A)−Cu(1)−Br(1)	113.45(9)
N(1)−Cu(1)−Br(1)	109.53(10)	N(2A)−Cu(1)−Br(1B)	101.50(11)
N(1)−Cu(1)−Br(1B)	102.25(11)	Br(1)−Cu(1)−Br(1B)	102.95(3)
Br(1)−Cu(2)−Br(2)	111.61(3)	Br(1)−Cu(2)−Br(2C)	111.83(3)
Br(2)−Cu(2)−Br(2C)	104.45(3)	Br(1)−Cu(2)−Br(2C)	117.80(3)
Br(2)−Cu(2)−Br(2D)	107.64(3)	Br(2B)−Cu(2)−Br(2D)	102.35(3)

All temperature-dependent X-ray powder experiments were performed in glass capillaries in static air atmosphere. Each pattern was measured every 5 °C (heating rate: 2 °C/min).

Differential Thermal Analysis, Thermogravimetry, and Mass Spectrometry. DTA−TG−MS measurements were performed simultaneously using the STA-409CD with Skimmer coupling from Netzsch, which is equipped with a quadrupole mass spectrometer QMA 400 (max 512 amu) from Balzers. The MS measurements were performed in analogue and trend scan mode, in Al_2O_3 crucibles under a dynamic helium (purity: 4.6) atmosphere using heating rates of 1 and 4 °C/min. All measurements were performed with a

(44) *STOE & CIE, X-Shape Version 1.03: Program for the crystal optimization for numerical absorption correction*; STOE & CIE GmbH: Darmstadt, Germany, 1998.
(45) *STOE & CIE, X-Red Version 1.11: Program for data reduction and absorption correction*; STOE & CIE GmbH: Darmstadt, Germany, 1998.
(46) Sheldrick, G. M. *SHELXS 97, Program for Crystal Structure Solution*; University of Göttingen: Göttingen, Germany, 1997.
(47) Sheldrick, G. M. *SHELXL-97, Program for the Refinement of Crystal Structures*; University of Göttingen: Göttingen, Germany, 1997.

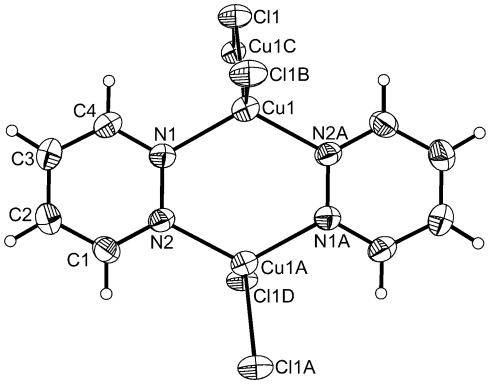

Figure 2. Crystal structure of catena[CuCl(μ_2-pyridazine-*N*,*N*)] (**I**) with labeling and displacement ellipsoids drawn at the 50% probability level (symmetry operations: A, $-x+2$, $-y+1$, z; B, $x+1$, y, z; C, $x-1$, y, z; D, $-x+1$, $-y+1$, z).

flow rate of 75 mL/min and were corrected for buoyancy and current effects.

Differential Scanning Calorimetry. DSC experiments were performed with the DSC 204/1/F from Netzsch in closed and open Al crucibles with heating and cooling curves of 3 °C/min. The calorimeter was calibrated using standard reference substances. All characteristic temperatures were estimated from different measurements at 3 °C/min.

Elemental Analysis. C, H, N analysis was performed using a CHN-O-RAPID combustion analyzer from Heraeus, and EDAX was performed using a Philips XL30 environmental scanning electron microscope (ESEM) with an EDAX system.

Results

Crystal Structures. The second modification of catena-[CuCl(μ_2-pyridazine-*N*,*N*)] (**I**) crystallizes in the triclinic space group $P\bar{1}$ with 2 formula units in the cell (Table 1). Each copper atom is coordinated by two symmetry equivalent chlorine and two nitrogen atoms of two pyridazine ligands related by a center of inversion (Figure 2). The Cu−Cl and Cu−N bond lengths are comparable to those of the polymorphic modification **LI**,[29] and the coordination polyhedron around the copper atoms can be described as a strongly distorted tetrahedron (Table 2). The copper atoms and the chlorine atoms form CuCl chains which run along the crystallographic *a*-axis (Figure 3: top). The copper atoms in each of two parallel CuCl chains are linked by two pyridazine ligands to discrete double chains. Within the chains the pyridazine ligands are coplanar oriented and are stacked in the direction of the chain axis (Figure 3: bottom).

This structure is completely different from that of form **LI**, in which $(CuCl)_2$ dimers occur which are connected into chains by the pyridazine ligands (Figure 1).

The crystal structure of **LI** can be derived formally from that of **I** cutting the CuCl−pyrazine chains into $(CuCl)_2$-$(pyrazine)_2$ units, which condense with units of neighboring chains (Compare Figure 1 with Figure 3: bottom). However, for this process large translational and rotational movements are necessary, and if a transformation of one form into the other can be observed, no smooth microscopic pathway can be expected.

From our thermal investigations (see below) on **LI** and **LII** we know that new amine-poorer 2:1 compounds exist.

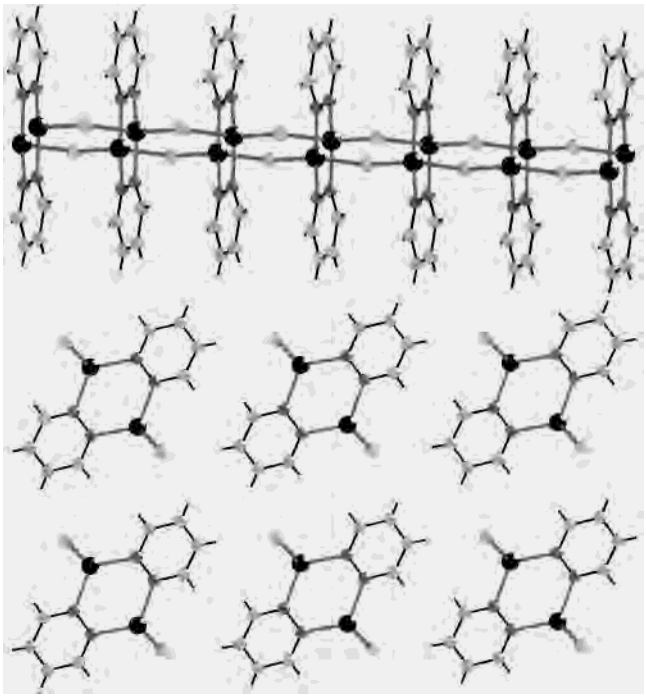

Figure 3. Crystal structure of catena[CuCl(μ_2-pyridazine-*N*,*N*)] (**I**) with view of the CuCl chains (top) and in the direction of the crystallographic *a*-axis (bottom).

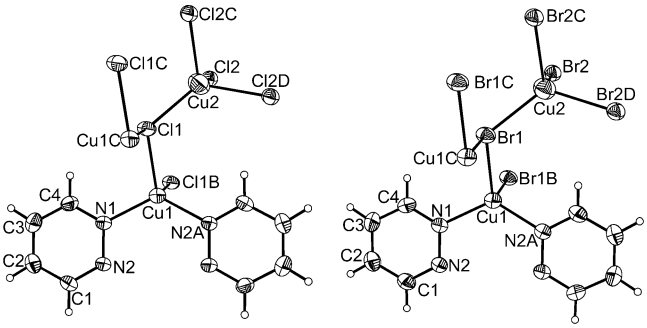

Figure 4. Crystal structure of poly[$(CuX)_2$(pyridazine-*N*,*N*)] (X = Cl (**II**; left), Br (**III**; right)) with labeling and displacement ellipsoids drawn at the 50% probability level (symmetry operations: A, $-x+1$, $-y+2$, $-z+1$; B, $x-1$, y, z; C, $x+1$, y, z; D, $x+2$, $y+2$, $z+2$).

Starting from these results we have succeed in growing single crystals for a structure determination.

Both compounds are isotypic and crystallize in the triclinic space group $P\bar{1}$ with 2 formula units in the unit cell (Table 1). The asymmetric unit consists of two crystallographically independent Cu and X atoms (X = Cl (**II**), Br (**III**)) as well as two crystallographically independent pyridazine ligands, all of them located in general positions (Figure 4). One copper atom (Cu1) is coordinated by two halide atoms as well as two nitrogen atoms from two pyridazine ligands, whereas the second copper atom (Cu2) is only surrounded by halide atoms (Figure 4). Both copper atoms are in a tetrahedral environment, and the coordination polyhedron around Cu2 is much more distorted than that around Cu1 (Table 2). In the crystal structure of these compounds a fascinating CuX substructure is found (Figure 5).

In this substructure CuX double chains are observed in a ladder-like arrangement that frequently occurs in such 2:1

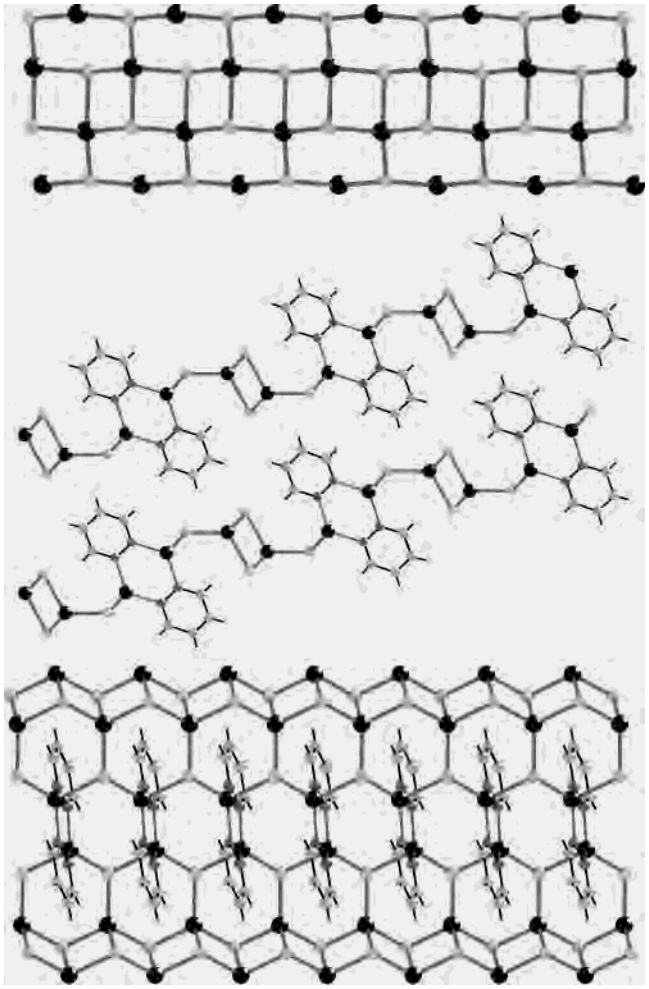

Figure 5. Crystal structure of poly[$(CuX)_2$(pyridazine-*N*,*N*)] (X = Cl (**II**), Br (**III**)) with view of the CuX substructure (top), view onto (100) (middle), and view onto (010) (bottom).

CuX coordination polymers. Normally, these double chains are linked by bidentate ligands into sheets. However, in compounds **II** and **III** the copper atoms within the double chains are only coordinated by halide atoms and are connected to two additional CuX single chains (Figure 5: top). From this arrangement tetrameric CuX chains are formed, which elongate in the direction of the crystallographic *a*-axis (Figure 5: middle). Whereas in the central CuX double chain nearly square $(CuX)_2$ units are found, the connection to the outer CuX single chains yields six-membered $(CuX)_3$ rings that are oriented perpendicular to the double chains. Each of the two outer copper atoms of neighboring chains are linked by two pyridazine ligands to form sheets that are parallel to (010) (Figure 5: bottom).

Crystallization Experiments. If a mixture of single crystals of the two polymorphic forms **I** and **LI** is stirred in acetonitrile for 1 day at room temperature and the residue is investigated by X-ray powder diffraction, it can be shown that all crystals of **LI** are transformed into crystals of **I**. Therefore, compound **I** is the most stable form at room temperature. If pure **I** is heated at 180 °C in sealed glass ampules, no transformation into **LI** is observed within several days, which demonstrates that **I** is also the most stable

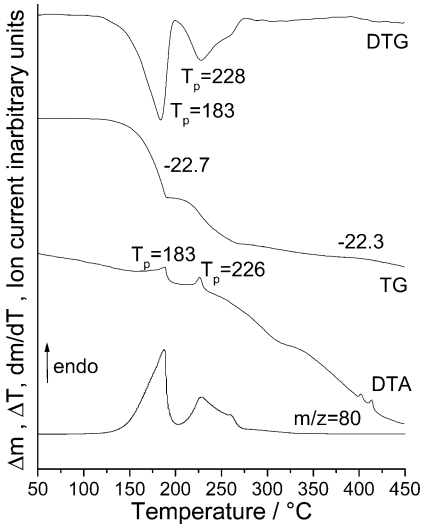

Figure 6. DTA, TG, DTG, and MS trend scan curves for catena[CuCl-(μ_2-pyridazine-*N*,*N*)] (**LI**) (weight = 18.90 mg; heating rate, 4 °C/min; given are the peak temperatures (T_p) in °C and the mass change in %; *m*/*z* (80) = pyridazine).

modification up to 180 °C. However, if this mixture is cooled to room temperature, also a few crystals of **LI** can be isolated. This is in agreement with the preparation conditions for **LI** reported by Sheldrick et al. in which the reaction was performed at higher temperatures and crystals of **LI** were isolated on slow cooling.[29] We believe that **LI** is formed by kinetic control and transforms into the most stable form **I**. It might be that this process needs some time in the case of single crystals and therefore crystals of **LI** can be isolated. This assumption is supported by kinetically controlled crystallization experiments. If a saturated solution of CuCl in acetonitrile is added to a solution of pyridazine in acetonitrile with stirring and the red precipitate is filtered off within seconds, X-ray powder diffraction proves that a microcrystalline powder of **LI** has formed which contains only minute amounts of the stable form **I**. In all experiments performed during this work we have never isolated phase pure samples of **LI**.

Thermoanalytical Investigations. On heating compound **LI** in a simultaneous DTA−TG−MS experiment, an endothermic event is observed at a peak temperature of about 183 °C which is accompanied with a mass loss in the TG curve of 22.7% (Figure 6). The experimental mass loss is in good agreement with that calculated for the removal of half of the pyridazine ligands (Δm_{theo}: $-{}^1/_2$pyridazine = 22.4%). Therefore, from the TG curve one can expect the formation of a 2:1 amine-poorer phase. This is proved by mass spectroscopy which shows that only pyridazine (*m*/*z* = 80) is emitted. On further heating a second mass loss is observed in which the remaining ligands are emitted. From the DTG curve it is obvious that both thermal events are well separated. X-ray powder diffraction proves that the final product of this reaction consists of CuCl.

If the reaction is stopped after the first mass loss at 207 °C and the residue is investigated by X-ray powder diffraction, it can be proven that the amine-poorer compound **II** has formed very pure (Figure 7). In addition, elemental

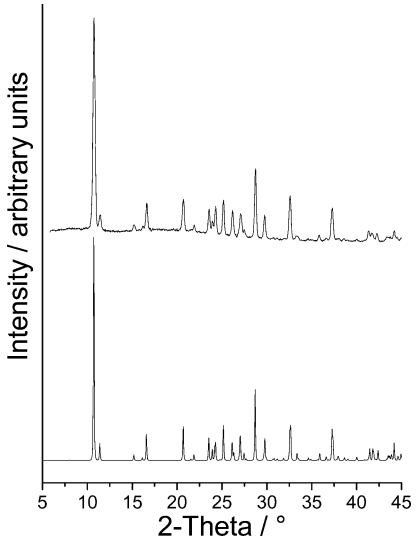

Figure 7. Experimental X-ray powder pattern of the residue isolated at 207 °C during the thermal decomposition of catena[CuCl(μ_2-pyridazine-*N*,*N*)] (**LI**) (top) and calculated X-ray powder pattern for the 2:1 compound poly[(CuCl)$_2$(pyridazine-*N*,*N*)] (**II**) (bottom).

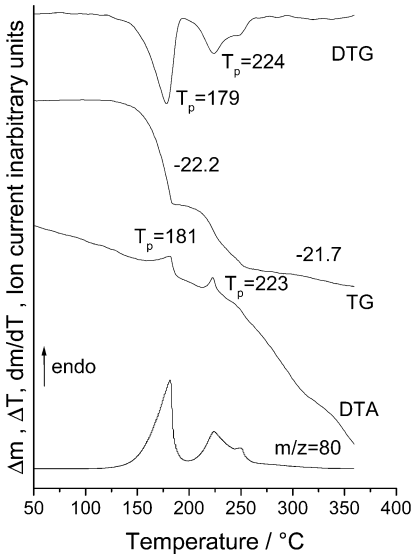

Figure 8. DTA, TG, DTG, and MS trend scan curves for catena[CuCl(μ_2-pyridazine-*N*,*N*)] (**I**) (weight = 26.3 mg; heating rate, 4 °C/min; given are the peak temperatures (T_p) in °C and the mass change in %; *m*/*z* (80) = pyridazine).

analysis of the residue is in good agreement with that calculated for this 2:1 compound from single-crystal data.

If the new modification **I** is heated in a thermobalance, a similar behavior as for **LI** is found (Figure 8). The first mass loss is in good agreement with that calculated for the removal of half of the pyridazine ligands. If the residue is isolated after the first mass step and is investigated by X-ray powder diffraction, one can prove that the 2:1 compound **II** has formed. From the DTA curves shown in Figures 6 and 8 there is no hint for a polymorphic phase transition. However, the energies involved in such transformations are often very low and cannot be detected by these experiments.

To investigate if additional phases or a polymorphic phase transition occurs during the thermal reactions of **I** and **LI**, experiments using temperature dependent X-ray powder

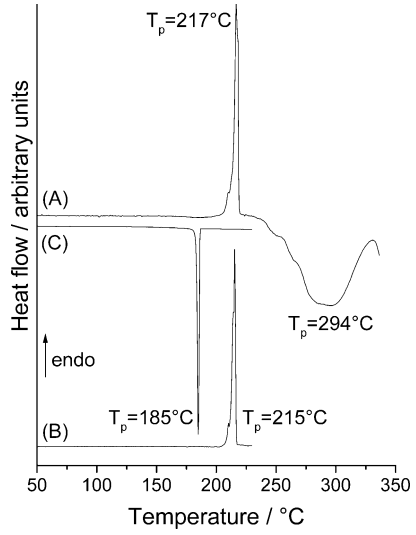

Figure 9. DSC curves for catena[CuCl(μ_2-pyridazine-*N*,*N*)]. (**I**) Heating curve to 350 °C (A), heating curve to 230 °C (B), and cooling to room temperature (C) (Al crucibles with hole; T_p = peak temperature).

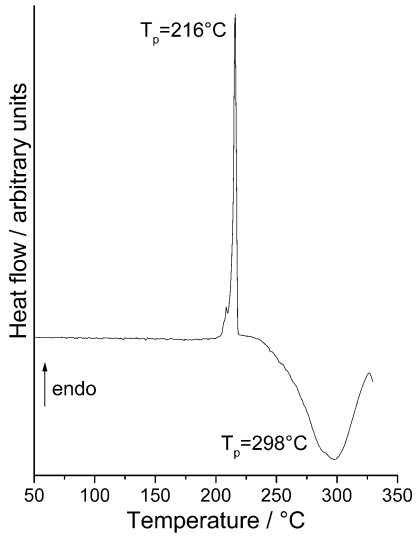

Figure 10. DSC curve for catena[CuCl(μ_2-pyridazine-*N*,*N*)] (**LI**) (Al crucibles with hole; T_p = peak temperature).

diffraction were performed. However, from these experiments there is no hint for additional intermediate phases or a polymorphic transition of one form into the other. In addition, the decomposition temperatures of both forms are identical within the error of this experiment.

The thermal behavior of both modifications was additionally investigated using differential scanning calorimetry (DSC) (Figures 9 and 10). If compound **I** is heated, an endothermic signal is measured at 217 °C that corresponds to the transformation into the amine-poorer 2:1 compound **II** (Figure 9: A). Compared to the DTA−TG measurements the decomposition temperature is shifted to a higher value. This can be ascribed to the different experimental conditions. In the DTA−TG−MS measurements the reaction products are transported out of the crucible by a continuous gas flow whereas in the DSC measurements static conditions and crucibles with a small hole are used. However, when the temperature is raised, compound **II** decomposes in an

exothermic reaction to CuCl, which was proven by X-ray powder diffraction. This is in contrast to the results of the DTA−TG measurements discussed above where both reactions (**I** → **II** → CuCl) are endothermic.

Obviously CuCl is much more stable than the 2:1 compound, which is expected because of its high heat of formation. This difference can also be ascribed to the different experimental conditions because in the DTA−TG measurements a large amount of the heating energy is needed for the vaporization of the ligand, which cannot happen in the DSC measurements. Therefore, the exothermic reaction is overcompensated, suggesting an endothermic formation of CuCl. This assumption is supported by an additional DSC experiment. If heating is stopped after the first endothermic event and the sample is cooled, an exothermic signal is observed in the DSC curve (Figure 9). The residue was identified as the starting compound **I**. Obviously, the ligand was not vaporized and the reaction of compound **I** into **II** is reversible under these conditions. To prove the assumptions made above, an additional DSC experiment was performed using open crucibles. In this case both steps are endothermic and the decomposition temperatures are comparable to those measured in the DTA−TG investigations. Because not all of the ligand is removed using static conditions, a small exothermic signal is measured after the second step.

If the second modification **LI** is investigated, a similar behavior as for form **I** is found (Figure 10).

We made several experiments for both modifications, and we have never found hints for a polymorphic transformation. In addition, the decomposition temperatures for both forms are comparable within the experimental error. Unfortunately, the decomposition energies cannot be compared because in all experiments a different amount of the ligand is vaporized. Therefore, the enthalpies are certainly wrong and equal within the experimental error. Therefore, no differences between both modifications can be detected.

When the bromine compound **LII** is heated in a thermobalance, a similar behavior as for compounds **I** and **LI** is found (Figure 11).

At about 200 °C a mass loss of 17.9% is found in the TG curve, which is in good agreement with that calculated for the removal of half of the pyridazine ligands (Δm_{theo}: $-{}^1/_2$pyridazine = 17.9%) (Figure 11). When the temperature is increased, a second mass loss of about 17.1% is observed, which corresponds to the complete removal of the remaining ligands. This assumption is supported by simultaneous MS measurements which show that only pyridazine (m/z = 80) is emitted. The residue of this reaction was identified as CuBr by X-ray powder diffraction. The DTG curve shows that both thermal events are well separated. Therefore, a second TG experiment was performed in which the reaction was stopped after the first mass loss had finished. In the X-ray powder diffraction of the residue the 2:1 compound **III** had formed very pure (Figure 12). In addition, elemental analysis of the residue is in good agreement with that calculated.

The TG curve for the bromine compound **LII** shows a smooth decrease after the formation of the 2:1 compound, and there seems to be an additional step before CuBr is formed. To be sure that no additional intermediate phase occurs during this reaction we have isolated several residues at different temperatures; but in all intermediate residues mixtures of the 2:1 compound and CuBr could be identified by X-ray powder diffraction. This result is further supported by experiments using temperature dependent X-ray powder diffraction which show that only a transformation of **LII** into **III** occurs, with decomposition directly to CuBr on further heating.

When compound **LII** was investigated by DSC measurements, similar observations were made as for the CuCl compounds **LI** and **I** (Figure 13). The transformation of **LII** into the amine-poorer 2:1 phase **III** occurs at 244 °C in an endothermic reaction and is reversible, and decomposition of **III** into CuBr is observed at about 303 °C in an exothermic reaction (Figure 13).

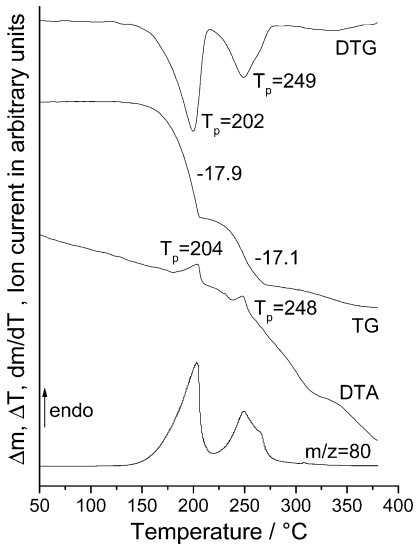

Figure 11. DTA, TG, DTG, and MS trend scan curves for catena[CuBr-(μ_2-pyridazine-*N*,*N*)] (**LII**) (weight = 25.51 mg; heating rate, 4 °C/min; given are the peak temperatures (T_p) in °C and the mass change in %; m/z (80) = pyridazine).

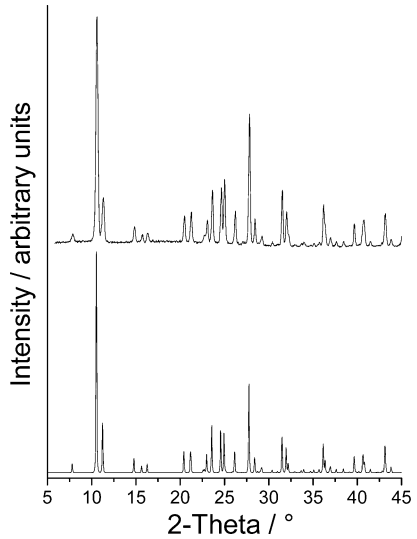

Figure 12. Experimental X-ray powder pattern of the residue isolated at 216 °C during the thermal decomposition of catena[CuBr(μ_2-pyridazine-*N*,*N*)] (**LII**) (top) and calculated X-ray powder pattern for the 2:1 compound poly[$(CuBr)_2$(pyridazine-*N*,*N*)] (**III**).

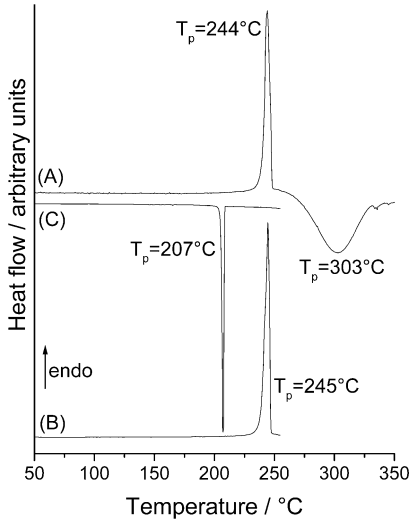

Figure 13. DSC curves for catena[CuBr(μ_2-pyridazine-*N*,*N*)] (**LII**). Heating curve up to 350 °C (A), heating curve up to 255 °C (B), and cooling to room temperature (C) (Al crucibles with hole; T_p = peak temperature).

Table 3. Selected Crystal Data for Catena[CuCl(μ_2-pyridazine-*N*,*N*)] (**I**), Catena[CuCl(μ_2-pyridazine-*N*,*N*)] (**LI**), and Catena[CuBr(μ_2-pyridazine-*N*,*N*)] (**LII**)[a]

	I	**LI**	**LII**
space group	$P\bar{1}$	*Cmca*	*Cmca*
a, Å	3.7512(6)	12.279(2)	12.336(3)
b, Å	8.412(1)	14.434(2)	14.805(4)
c, Å	8.900(1)	12.709(2)	13.055(6)
α, deg	90.43(1)		
β, deg	94.04(1)		
γ, deg	92.27(1)		
unit cell vol, Å^3	279.9(1)	281.6(2)	298.8(2)
calcd density, g cm^{-3}	2.125	2.112	2.491

[a] The lattice parameters were redetermined by us, and the unit cell volumes were recalculated for $Z = 2$.

Discussion

Concerning the thermodynamic stability of the two modifications the results of the crystallization experiments show clearly that form **I** should be the thermodynamically most stable form between room temperature and about 180 °C and that **LI** is metastable in this temperature range. Because the density of **I** is significantly higher than that of **LI** (Table 3), the former should also be more stable at lower temperatures.[17]

Modification **LI** can only be obtained by kinetic control and transforms within a short time into the stable form **I**. In this context it must be noted that in the beginning of our investigations we have frequently isolated samples at room temperature that contain a large amount of the metastable form **LI** whereas after some weeks practically all samples contain pure **I**. The only possibility for the preparation of **LI** was the crystallization by kinetic control within seconds. It might be that after some time the equipment in the laboratory is contaminated with crystals or nuclei of the thermodynamically most stable modification and, therefore, the preparation of the metastable form is difficult to achieve. Such funny phenomena are well-known and several examples for this are enjoyably described in ref 48. However, the crystallization experiments performed show only a transformation of the thermodynamically metastable form **LI** into the stable form **I**, whereas the opposite transformation was never observed. Hence, we assume that both modifications behave in a monotropic fashion. It might be that **LI** becomes more stable at higher temperatures, e.g., directly before decomposition. But this we have investigated only up to 180 °C. In addition, besides our crystallization experiments we have no hints for the transformation of one form into the other in the solid state. Assuming that both forms behave in a monotropic fashion, one would expect a polymorphic transition of form **LI** into **I** on heating, which presumably should proceed via an exothermic reaction. However, it might be that this transition is suppressed by the solid state kinetics.

Concerning the structural aspects of the dimorphism it is difficult to decide why form **I** is more stable than form **LI**. It might be that this is correlated with the CuX substructure because in most of such CuX coordination polymers single or double chains are observed whereas (CuCl) dimers like in **LI** are rare. In this context it must be noted that the corresponding 1:1 compound with CuBr, which seems to be the only modification, is isotypic to **LI**. However, even in this case one can argue in a similar way. For CuI several compounds with such CuX dimers are known and, therefore, one can assume that the tendency for the formation of smaller CuX units increases from Cl to I. Nevertheless, because the structures of the coordination compounds with CuCl are often identical to those with CuBr, one can expect the existence of a second modification for the CuBr compound **LII** which would be probably isotypic to **I** (Table 3). Therefore, we have made several experiments in order to obtain a second modification but without any success. In one experiment we have used crystals of the CuCl compound **I** as a template for the growth of an isotypic CuBr compound, but the powder pattern can be sufficiently explained on the basis of a mixture of **I** and **LII**. This demonstrates the difficulty of drawing structure−property relationships even for compounds which are structurally strongly correlated.

Concerning the transformation of the 1:1 compounds **LI**, **I**, and **LII** into the new amine-poorer compounds **II** and **III** we have demonstrated that several different methods should be applied. In this context one should keep in mind that dependent on the experimental conditions different results are obtained. However, we have demonstrated again the power of thermal decomposition reactions for the discovering and the preparation of new coordination polymers. In the present work we isolated the 2:1 compounds **II** and **III** for the first time in our TG experiments. On the basis of these results we prepared **II** and **III** via the solution route. However, single crystals can be easily grown in solution but we have found no method to prepare phase pure samples.

Conclusions

In the present contribution we have demonstrated that polymorphism or isomerism is frequently observed even for coordination polymers and, therefore, this phenomenon should be always kept in mind in all strategies for the construction of new coordination frameworks. Concerning

(48) Dunitz, J. D.; Bernstein, J. *Acc. Chem. Res.* **1995**, *28*, 193−200.

the thermodynamic stability of all phases we have shown that it can change dramatically if one of the building blocks is exchanged. The same was found for other coordination polymers with similar topology but slightly different ligands.[24] However, for a deeper understanding for a more rational crystal design, such investigations are helpful and therefore really needed. For the discovery of new compounds, their polymorphs, or isomers, also typical solid state reactions like the thermal decomposition presented above should be used. This is impressively demonstrated in a further contribution.[49]

Acknowledgment. We gratefully acknowledge the financial support by the State of Schleswig-Holstein. We are very thankful to Professor Dr. Wolfgang Bensch for financial support and the facility to use his experimental equipment.

Supporting Information Available: Lists with details of the structure determination, atomic coordinates, isotropic and anisotropic displacement parameters, CIF files, and drawings of the two structures as well as the results of the temperature-dependent X-ray powder measurements. This material is available free of charge via the Internet at http://pubs.acs.org.

IC026181I

(49) Näther, C.; Jess, I. *Inorg. Chem.*, submitted.